Electronic Supplementary Material (ESI) for ChemComm.

Supporting Information For:

Electropolymerization in a Confined Nanospace: Synthesis of PEDOT Nanoparticles in Emulsion Droplet Reactors

Myoung Won Lee[1], Deok-Jin Kwon[2], Junmo Park[1], Jae-Chul Pyun[2], Young-Joo Kim[2], and Hyun S. Ahn[1,*]

Contribution from: [1]*Department of Chemistry, Yonsei University, 50 Yonsei-ro, Seodaemun-gu, Seoul, 03722 Republic of Korea*
[2]*Department of Mechanical Engineering, Yonsei University, 50 Yonsei-ro, Seodaemun-gu, Seoul, 03722 Republic of Korea*

Email: ahnhs@yonsei.ac.kr

Table of Contents	**Page**
Experimental	S2
SEM Images PEDOT Prepared by Cyclic Voltammetry Method (**Figure S1**)	S3
In-situ Monitoring of PEDOT NP Synthesis by Chronoamperometry: 350 nm Droplet Reactors (**Figure S2**)	S4
In-situ Monitoring of PEDOT NP Synthesis by Chronoamperometry: 450 nm Droplet Reactors (**Figure S3**)	S5
Calculation of the Frequency of Droplet Collision Events on an Electrode	S6
Emulsion Droplet Collision Frequencies: Theory and Experiment (**Table S1**)	S6
Transmission Electron Microscopy Image of PEDOT NPs (**Figure S4**)	S7
Scanning Electron Micrographs of 40 nm PEDOT NPs (**Figure S5**)	S8
Scanning Electron Micrographs of 70 nm PEDOT NPs (**Figure S6**)	S9
Dynamic Light Scattering Plots of 60 and 100 nm Droplets (**Figure S7**)	S10
Electrosynthesized PEDOT NPs Dispersed in Water: Photograph (**Figure S8**)	S11
UV-vis Spectra of PEDOT:PF_6 NPs (**Figure S9**)	S12
Raman Spectra of PEDOT:PF_6 NPs (**Figure S10**)	S13
Assignment of Raman Features in PEDOT:PF_6 NPs (**Table S2**)	S14
Scanning Electron Micrographs of 350 and 450 nm PEDOT NPs (**Figure S11**)	S15
OLED Device Luminescence: Commercial PEDOT:PSS and Electrosynthsized PEDOT:PF_6 Comparison (**Figure S12**)	S16
UV-vis Spectra of PEDOT NP Decorated Anodes After Various Mechanical Stimuli (**Figure S13**)	S17
Long Term Stability of PEDOT NP based Supercapacitor Electrode by Cyclic Voltammetry (**Figure S14**)	S18
References	S19

Experimental

General. All aqueous solutions were prepared by use of ultrapure water (Youngin Ins. Aquapuri5: 18.2 MΩ, 3 ppm total oxidizable carbon). 2,3-Ethylenedioxythiophene (EDOT, > 98 % GC), Tetrabutylammonium Hexafluorophosphate ($TBAPF_6$, > 98 %), Sodium Hexafluorophosphate ($NaPF_6$, > 98 %), and Hydrogen peroxide (H_2O_2, 35 % in water) were purchased from TCI. Sorbitan Monooleate (Span® 80, ≥ 60 %, GC), Polyoxyethylene sorbitan monooleate (Tween®80, BioXtra) 1,3,5-Tri(m-pyridin-3-ylphenyl)benzene (TmPyPB, 98 %, HPLC), Tris[2-phenylpyridinato-C2,N]iridium(III) ($Ir(PPY)_3$),99 %) were purchased from Sigma-aldrich. Dichloromethane (LP Grade) was purchased from SK Chemicals. Sulfuric acid (H_2SO_4, 98 %) and Isopropyl alchohol (IPA, 99.9 %) were purchased from DAEJUNG. Poly(9-vinylcarbazole) (PVK, Mw > 100,000, GPC) and 1,3-Bis[2-(4-tert -butylphenyl)-1,3,4-oxadiazo-5-yl]benzene (OXD-7, > 99 %, GC) were purchased from Lumtec.

All electrochemical measurements were analyzed using a CH Instrument (Austin, TX) model 760E potentiostat. Glassy carbon plate (5 mm × 10 mm, Dasom RMS), Glassy carbon disc electrode (GC, 2 mm diameter, CH Instruments Inc.), Carbon ultramicroelectrode (UME, 10 μm diameter), and Indium tin oxide (ITO, 10 mm × 10 mm, 170 nm thickness, 9 $\Omega\ \mathrm{cm}^{-1}$) were used as working electrodes. Reference electrode employed was Ag/AgCl (0.2 V vs. Fc/Fc^+) and Pt wire was used as the counter electrode.

Dynamic light scattering (DLS, ELSZ-2000, Otsuka) was used for size measurement of organic nanodroplets. Absorption spectra in the UV-vis-NIR range was collected on a JASCO V-770 spectrometer, with the sample being injected solid phase mounted on an ITO substrate. Raman spectroscopy system was composed of a monochromator (Triax 320, f = 320 mm, Horiba Jobin-Yvon) with grating (1800 grooves/mm), a diode-pumped solid state laser (532 nm, spot size less than 1 μm, 3 mW laser beam power, 3 s accumulation time) and a Si array CCD (1024 × 256 picels on 26 × 26 μm^2, Horiba Jobin-Yvon). Scanning electron microscopy (SEM) was performed using a JEOL 7612f-plus with an accelerating voltage of 15 kV.

Synthesis of emulsion nanodroplets. An emulsion precursor solution was made by dissolving 25 mM EDOT and 0.2 M $TBAPF_6$ in dichloromethane. For the preparation of 200 nm droplets, 300 μL of emulsion precursor solution was mixed with 45 μL Span80 and 45 μL Tween80, and then added to 4.61 mL of water (including 0.1 M $NaPF_6$). The mixture was placed in a 15 mL conical tube, vortexed for 30 s, and then was pulsed with a ultrasonicator (VibraCell VC-505, SONICS, 500 W, amplitude 40%, 3 mm microtip) for 24 cycles with 5 s on, 5 s off pulse mode. Other ratios were required for emulsions of different sizes: 350 nm (600 μL precursor solution, 60 μL Span80, 60 μL Tween80, and 4.28 mL water), 450 nm (600 μL precursor solution, 10 μL Span80, 10 μL Tween80, and 4.38 mL water), and 600 nm (600 μL precursor solution, 2.5 μL Span80, 2.5 μL Tween80, and 4.40 mL water).

Fabrication of organic light emitting diode device. In order to create an OLED device, an ITO anode (5 mm × 5 mm) was deposited with 40 nm and 70 nm $PEDOT:PF_6$ nanoparticles as a hole transport layer and rinsed with water and acetone. Then, PVK:OXD-7:$Ir(PPY)_3$ (PVK:OXD-7 ratio = 60 : 40; $Ir(ppy)_3$ = 2 wt% of PVK:OXD-7) was mixed in chlorobenzene and stirred at 80 ℃ for 6 h. It was spin-coated to 80 nm thickness on the anode at 4000 rpm for 30 s and annealed at 100 ℃ for 1 h. A 50 nm thick TmPyPB electron transport layer was spin-coated at 5000 rpm for 30 s and dried at 80 ℃ for 30 min. Finally, 100 nm thick aluminum was sputtered on the TmPyPB layer under high vacuum condition as a cathode (less than 10^{-5} Torr). Voltage was applied from 0 to 30 V to the OLED device and luminance was measured on a spectroradiometer (CS-2000). The OLED device architecture employed here was similar to that in reference S1 (HTL) and S2 (EML and ETL).

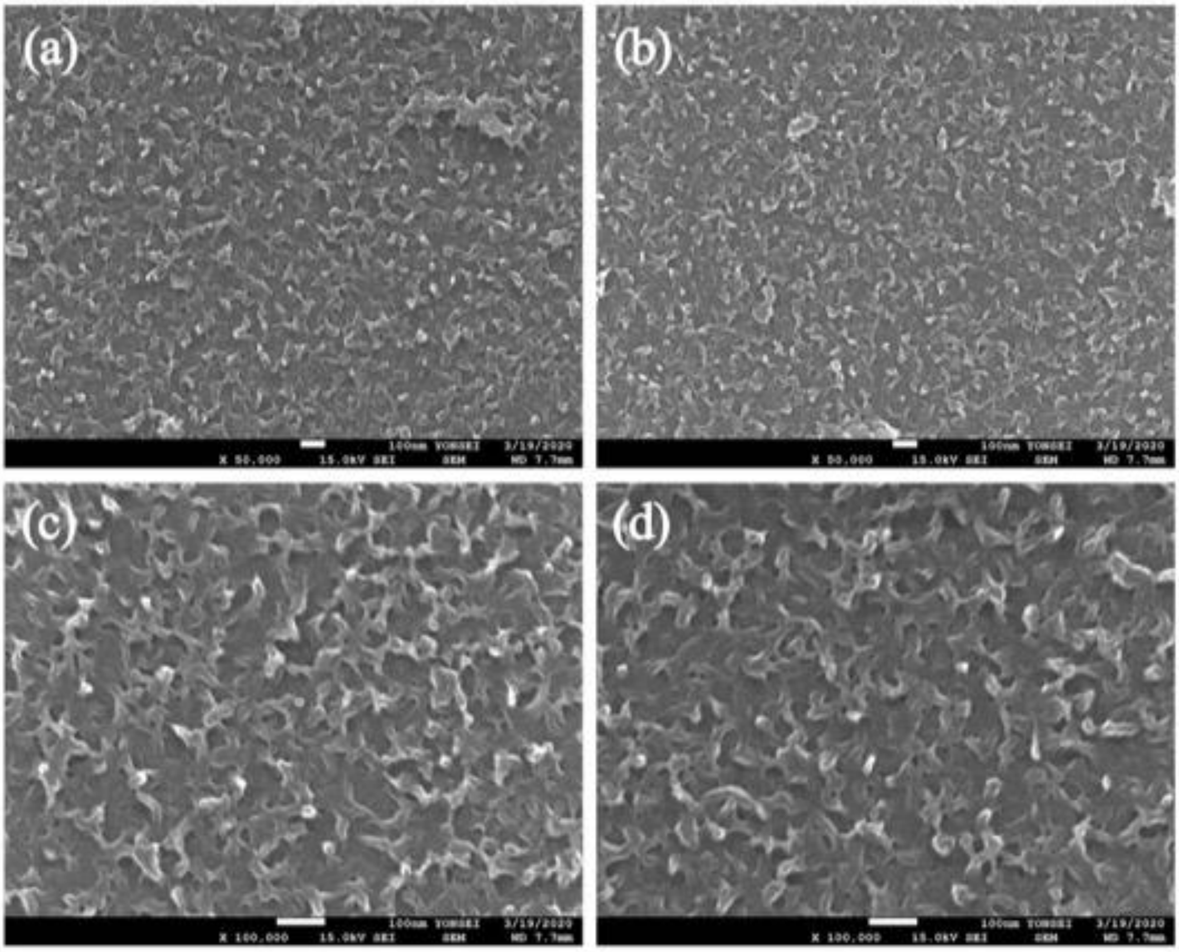

Figure S1. Scanning electron micrographs of PEDOT films electrosynthesized by cyclic voltammetry method (scanned from 0.3 V to 1.15 V). Typical for cyclic voltammetry synthesized PEDOT material, the film covered the entire electrode area. Scale bars are 100 nm in all images.

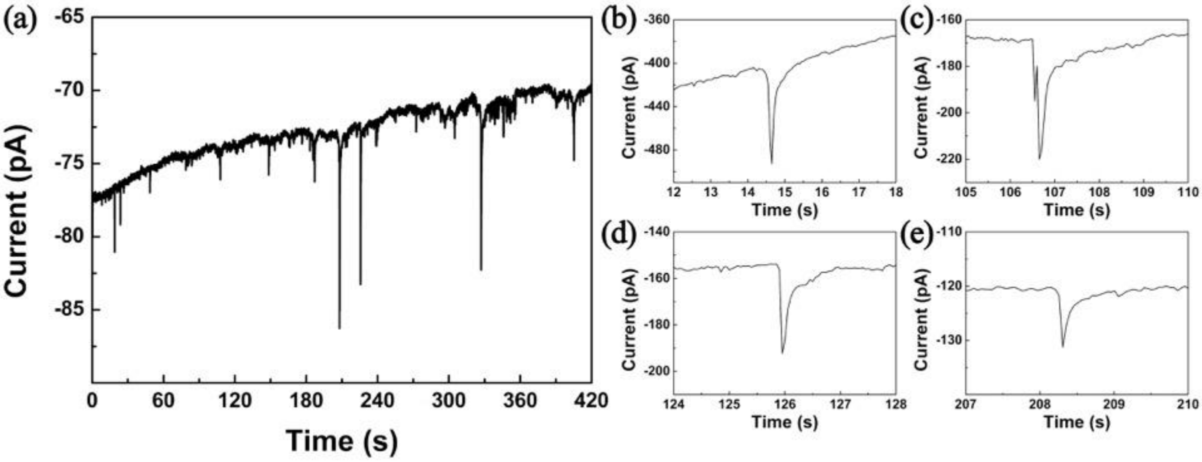

Figure S2. (a) Chronoamperogram of collision signals of 350 nm emulsion nanodroplets containing 25 mM EDOT on a 10 μm carbon UME. **(b)** – **(e)** Spike-like single droplet collision signals, each corresponding to synthesis of a PEDOT NP.

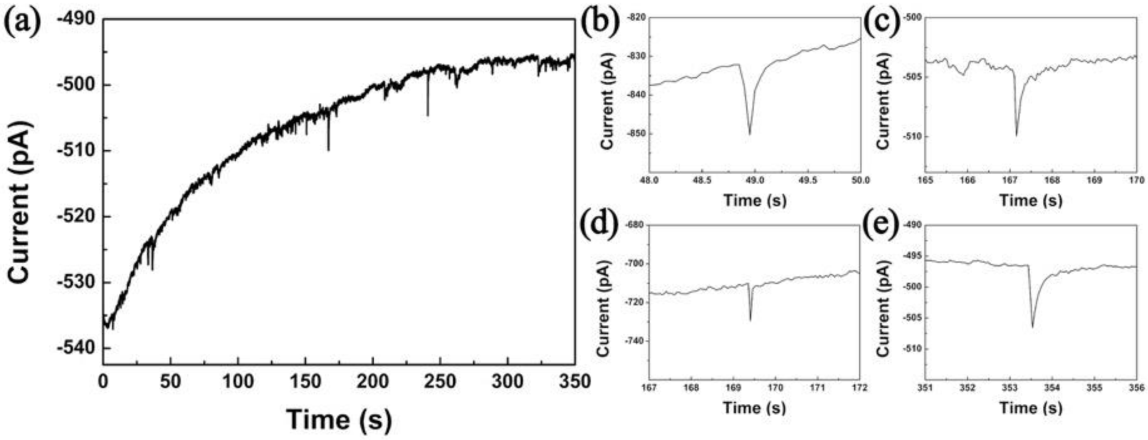

Figure S3. (a) Chronoamperogram of collision signals of 450 nm emulsion nanodroplets containing 25 mM EDOT on a 10 μm carbon UME. **(b)** – **(e)** Spike-like single droplet collision signals, each corresponding to synthesis of a PEDOT NP.

Calculation of Expected Collision Frequency of Emulsion Droplet Reactors

Emulsion droplet collision frequency on an electrode was predicted by estimation of the diffusion coefficient of nanodroplets in aqueous continuous phase from the Stokes-Einstein equation.[S2] An example calculation is as follows:

$$D_{200nm} = \frac{k_B T}{6\pi\eta r_{200\,nm}}$$

$$D_{200\,nm} = \frac{(1.381 \times 10^{-23}\ kg \cdot m^2 \cdot s^{-2} \cdot K^{-1}) \times (298\ K)}{6\pi \times (9.0 \times 10^{-4}\ kg \cdot m^{-1} \cdot s^{-1}) \times (1.00 \times 10^{-7}\ m)} = 2.4 \times 10^{-12}\ m^2 s^{-1}$$

$$C_{200\,nm} = \frac{\frac{V_{DCM}}{V_{200\,nm}}}{N_A} \cdot \frac{1}{V_s} = \frac{\frac{3 \times 10^{-7}\ m^3}{\frac{4}{3}\pi \times (1.00 \times 10^{-7}\ m)^3}}{(6.022 \times 10^{23})} \times \frac{1}{0.005\ L} = 2.38 \times 10^{-8}\ M$$

$$f_{200\,nm} = 4 \times D_{200\,nm} \times C_{200\,nm} \times r_{elec} \times N_A$$

$$= 4 \times (2.4 \times 10^{-12}\ m^2 \cdot s^{-1}) \times (2.38 \times 10^{-8}\ mol \cdot m^{-3}) \times (5 \times 10^{-6}\ m) \times (6.022 \times 10^{23}\ mol^{-1}) = 0.7\ s^{-1}$$

For droplets of 200 nm diameter, calculated collision frequency is *ca.* 0.7 Hz. Similarly, estimated frequencies of collision were 0.15 Hz for 350 nm, 0.054 Hz for 450nm, and 0.017 Hz for 650 nm droplets. Experimentally observed frequencies of collision events agreed reasonably with that theoretically estimated (considering the stochastic nature of these events based on Brownian random walk), and are tabulated in Table S1 below.

Table S1. Theoretically calculated emulsion droplet collision frequencies and those observed experimentally (for 200, 350, and 450 nm droplets colliding on a 10 μm UME).

	200 nm	**350 nm**	**450 nm**
Theoretical collision frequency	0.7	0.15	0.054
Experimental collision frequency	0.14	0.04	0.02

Electrodes decorated with PEDOT NPs in supercapacitor and OLED applications were also prepared based on calculations shown above. Reaction times for NP synthesis were chosen according to the calculated frequency and the desired number of particles for each application. For example, supercapacitors in Figure 3b were prepared with reaction times within 60 minutes to ensure good coverage of the substrate electrode without overloading it with PEDOT. The 60-minute data point for 200 nm sample expects approximately 2000 NPs (corresponding to 100 % coverage of the electrodes with PEDOT NP), and experimentally 2520 NPs were deposited to fabricate the device on which capacitance measurements were performed. Similarly, for 350 and 450 nm NP capacitors, 532 and 146 NPs, respectively were deposited to yield supercapacitors that were tested. Similar consideration was taken into account for the preparation of OLED anode.

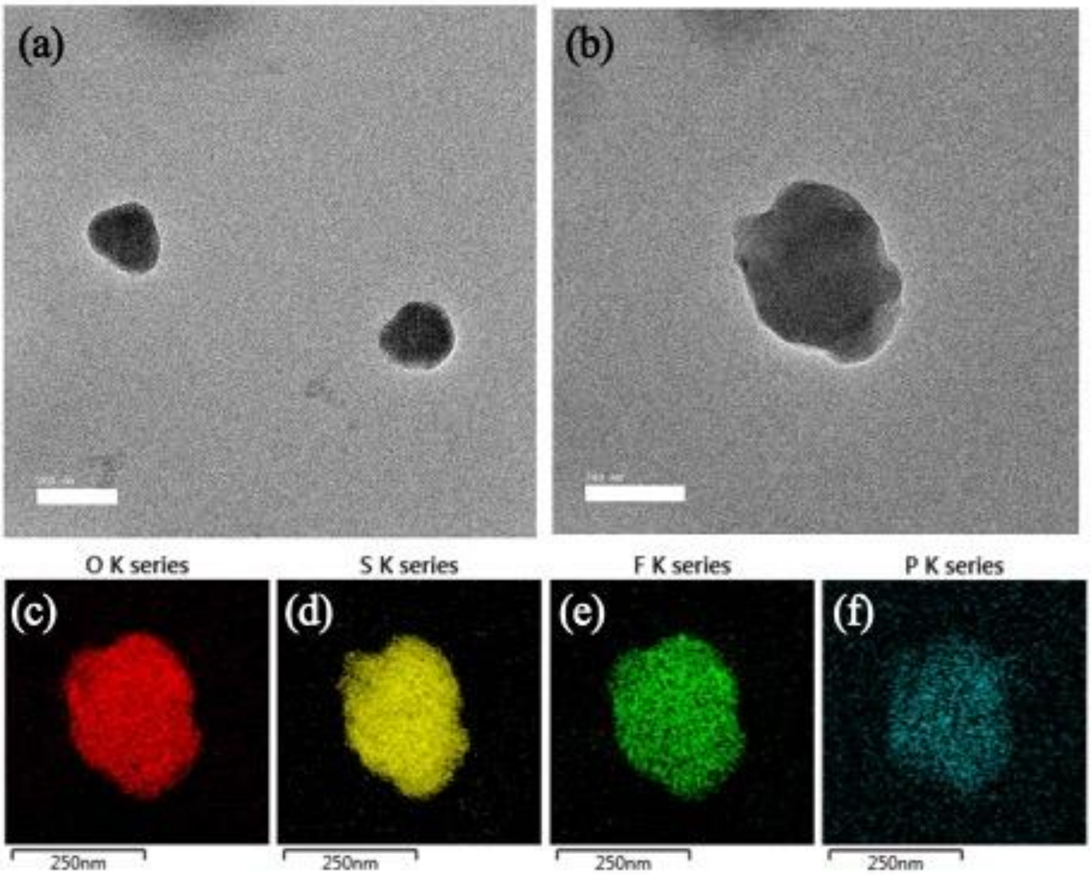

Element	Wt%	Wt% Sigma	Atomic %
O	39.9	0.44	54.40
F	9.9	0.34	11.47
P	1.40	0.22	0.99
S	48.72	0.43	33.14
Total	100.00		100.00

Figure S4. (a),**(b)** Transmission electron micrographs of PEDOT NPs synthesized by the droplet-collision electrochemistry. Generally spherical morphology was observed. **(c)-(f)** Elemental maps of the PEDOT NPs with O, S, F, and P, respectively. Approximate composition remained true to that of PEDOT, with excess positive charge compensated by PF_6 anions, suggesting that the NPs synthesized in this work were PEDOT:PF_6. Scale bar in image **(a)** is 200 nm, and all other scale bars are 250 nm in length.

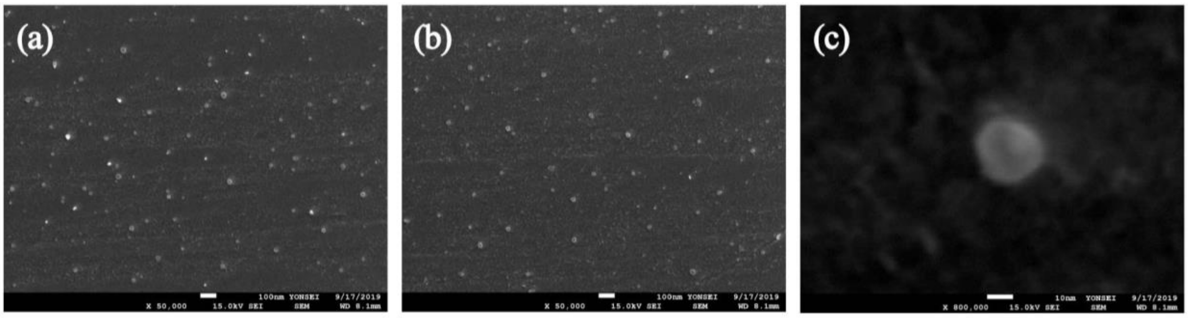

Figure S5. Scanning electron micrographs of 40 nm PEDOT NPs synthesized in 60 nm emulsion droplet reactors. Scale bars are 100 nm long in **(a)** and **(b)**, and 10 nm in image **(c)**.

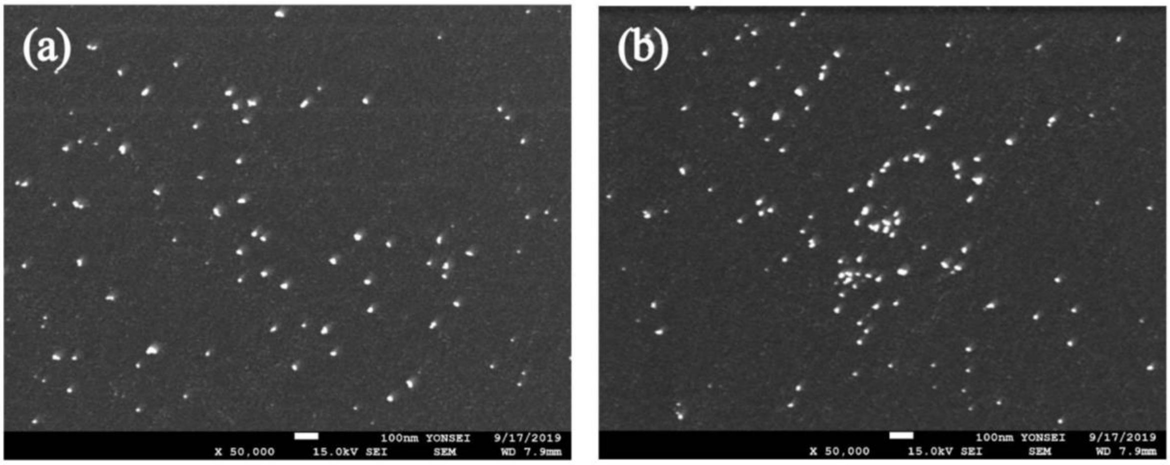

Figure S6. Scanning electron micrographs of 70 nm PEDOT NPs synthesized in 100 nm emulsion droplet reactors. Scale bars are 100 nm in length.

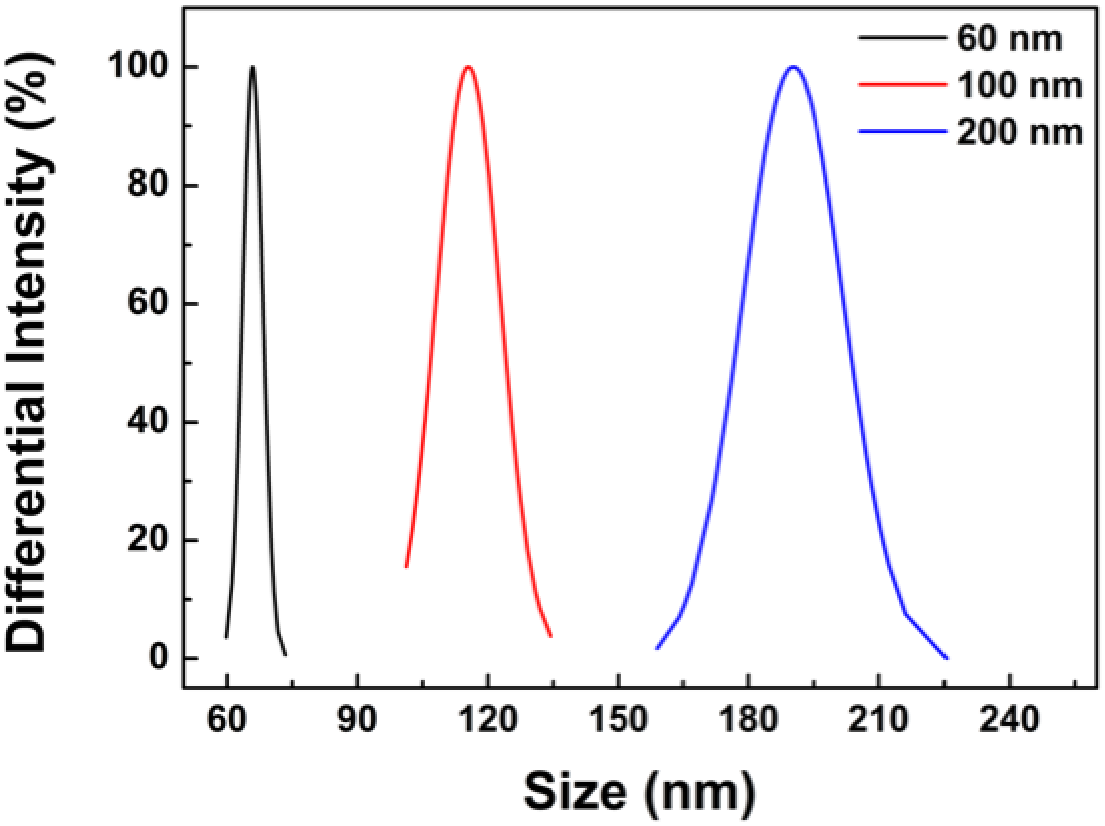

Figure S7. Distributions of droplet size measured by dynamic light scattering (60 nm-black, 100 nm-red, and 200 nm-blue).

Figure S8. Photograph of electrosynthesized PEDOT NPs (200 nm) dispersed in water. The synthesized NPs were electrode-bound strongly, however, with appropriate stimulation (ultrasonication) detachable and re-dispersible in solvent for further processing.

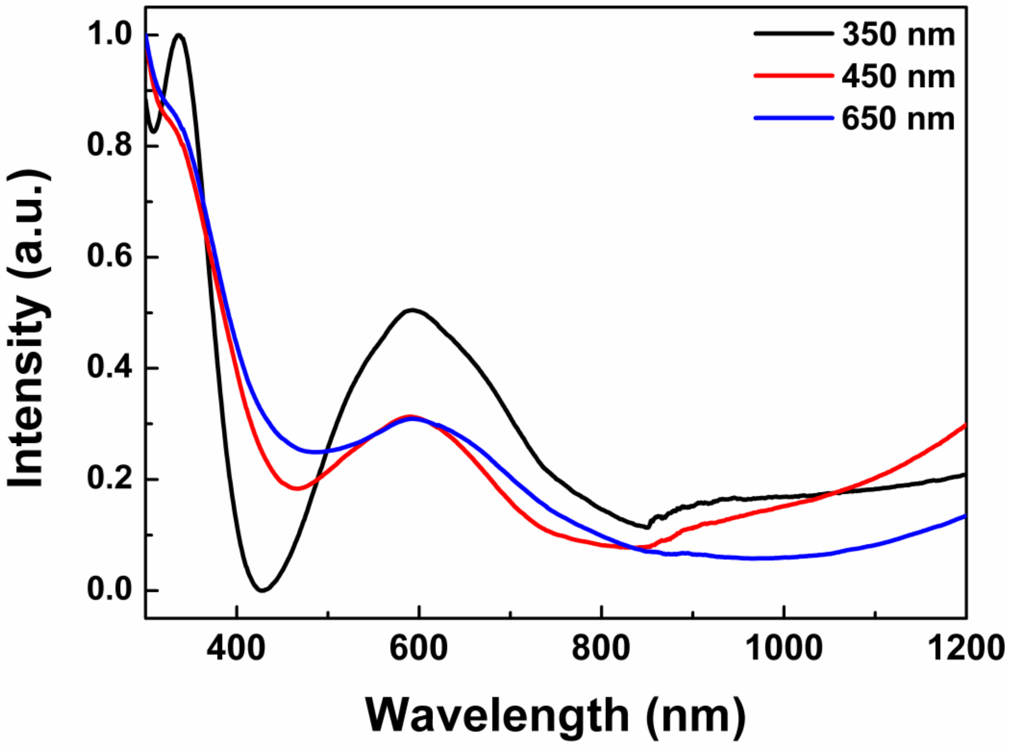

Figure S9. UV-vis spectra of PEDOT:PF_6 NPs (350 nm-black, 450 nm-red, and 650 nm-blue). Broad bands centered at 350 nm and 580 nm are characteristic of PEDOT:PF_6.

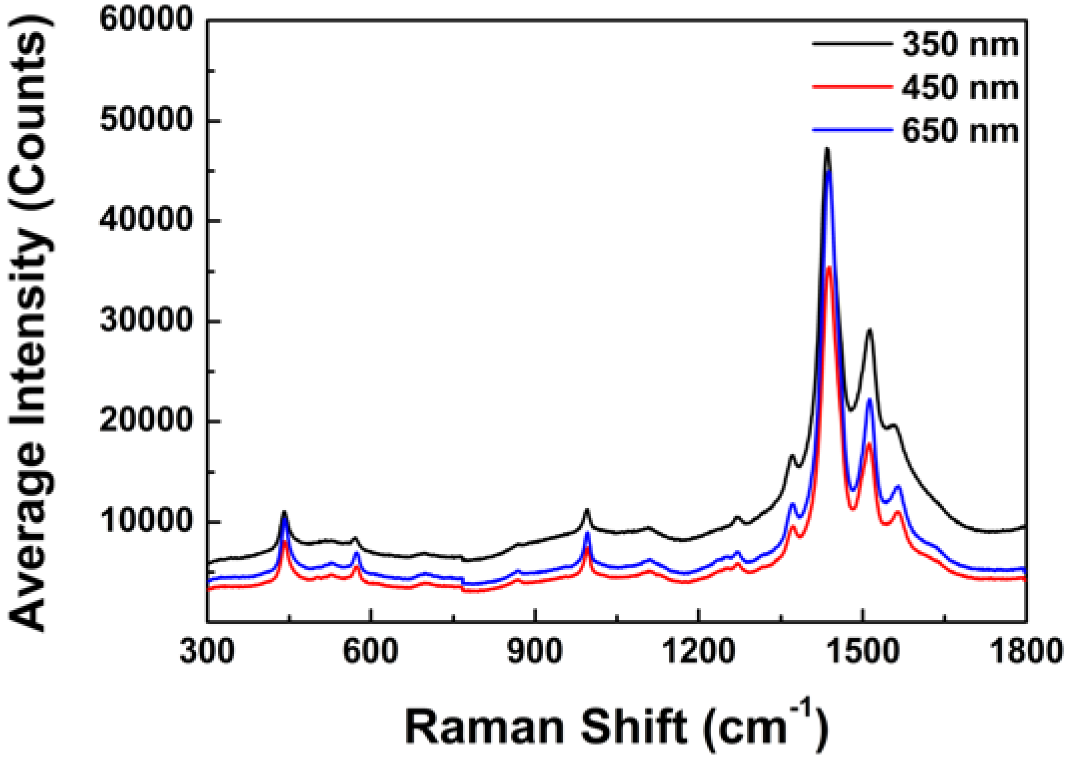

Figure S10. Raman spectra of PEDOT:PF_6 NPs (350 nm-black, 450 nm-red, and 650 nm-blue). Signature bands were observed corresponding to structural motifs in PEDOT. Peak assignments are tabulated below in Table S2.

Table S2. Raman peak assignments of the structural motifs in PEDOT:PF_6.

Peak Assignment	**Raman Shift Wavenumber (cm^{-1})**	
	Reference[S3,S4]	This Work
Asymmetric $C = C$ stretches	1520	1508
Symmetric $C_\alpha = C_\beta$ (-O) stretches	1431	1430
$C_\beta - C_\beta$ stretches	1369	1361
$C_\alpha - C_{\alpha'}$ (inter-ring) stretches	1270	1260
C-O-C deformation	1111	1100
Oxyethylene ring deformation	991	990
Symmetric C-S-C deformation	692	691
Oxyethylene ring deformation	440	440

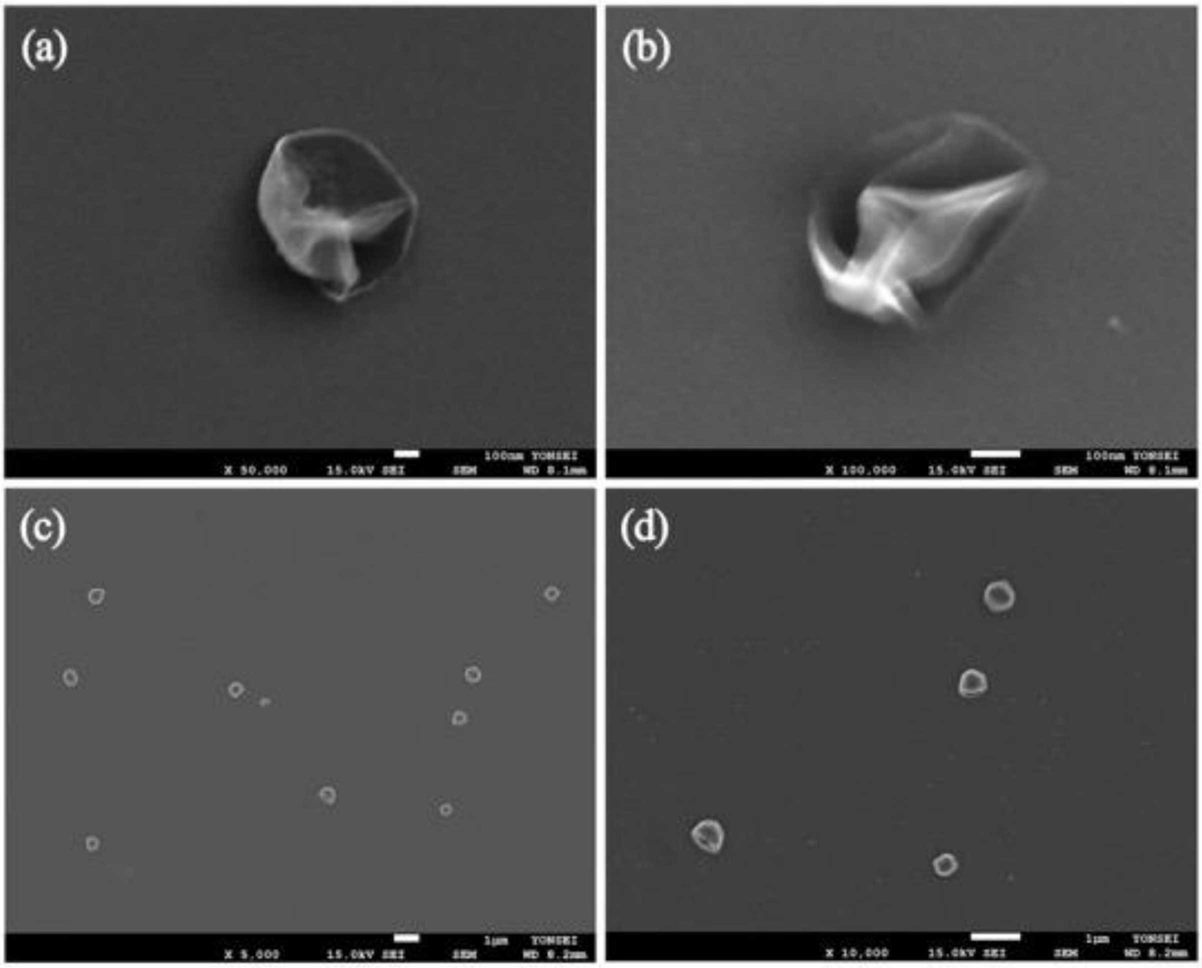

Figure S11. Scanning electron micrographs of 350 nm (**(a)**,**(c)**) and 450 nm (**(b)**,**(d)**) PEDOT NPs exhibiting partially hollow (shriveled) morphology. Scale bars are 100 nm in length for images in **(a)**, **(b)** and 1 μm in images **(c)**, **(d)**.

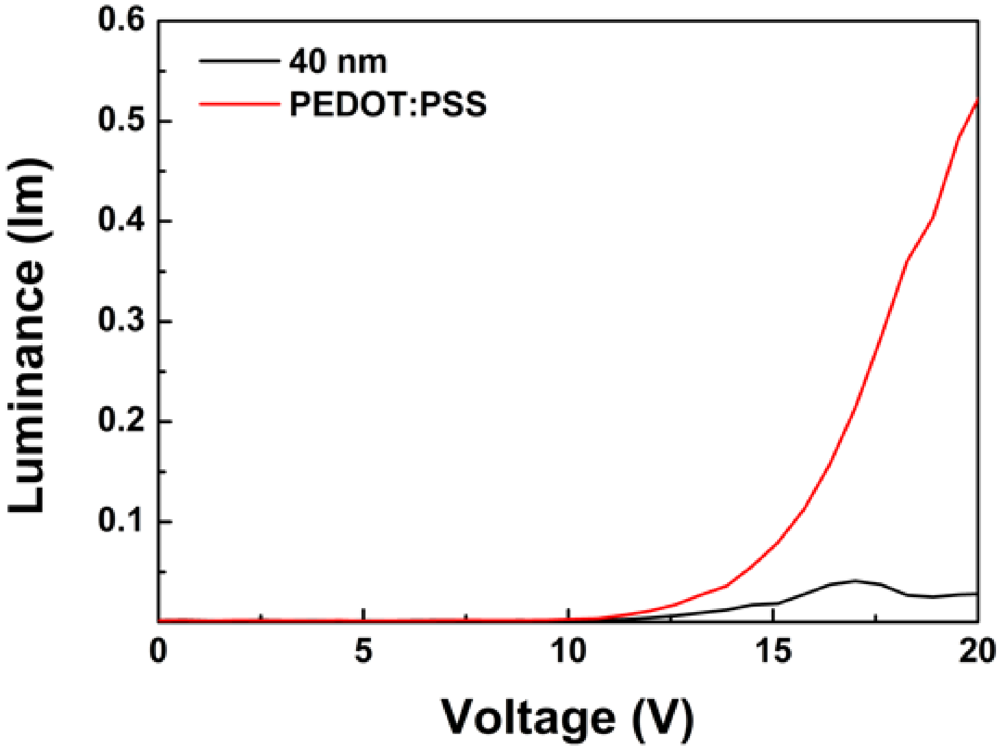

Figure S12. OLED device luminescence diagrams adopting 40 nm PEDOT:PF_6 NPs as a hole conducting layer (black) and that employing commercial PEDOT:PSS film (40 nm thick) as a hole conducting layer (red). The device implementing PEDOT:PF_6 NPs exhibited *ca.* 10 % performance compared to that with commercial PEDOT:PSS film.

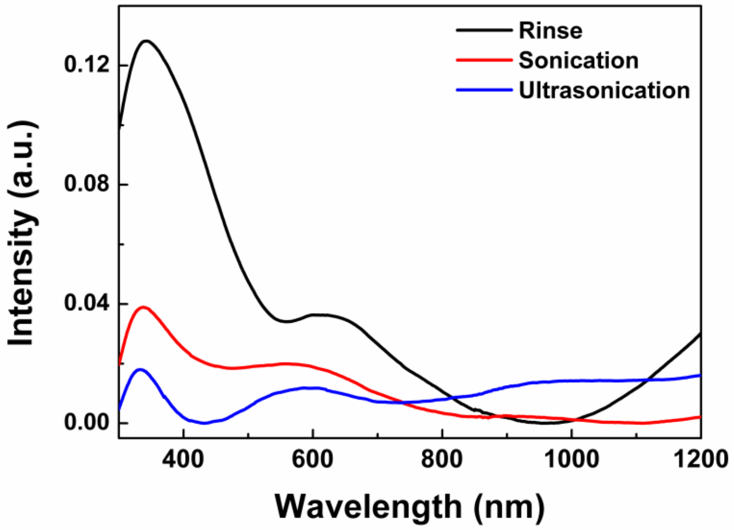

Figure S13. UV-vis spectra of PEDOT NP decorated electrodes. After multiple rinse cycles, the spectrum (black) exhibited no signs of decrease in intensity, suggesting that the PEDOT NPs adhere to the electrode (ITO) surface strongly. After water bath sonication (30 min; red trace) absorption band at 600 nm diminished dramatically, suggesting that upon bath sonication PEDOT NPs detach from the electrode. After ultrasonication (horn type; blue trace) the absorption diminished further, indicating that the PEDOT NPs were lost from the ITO electrode.

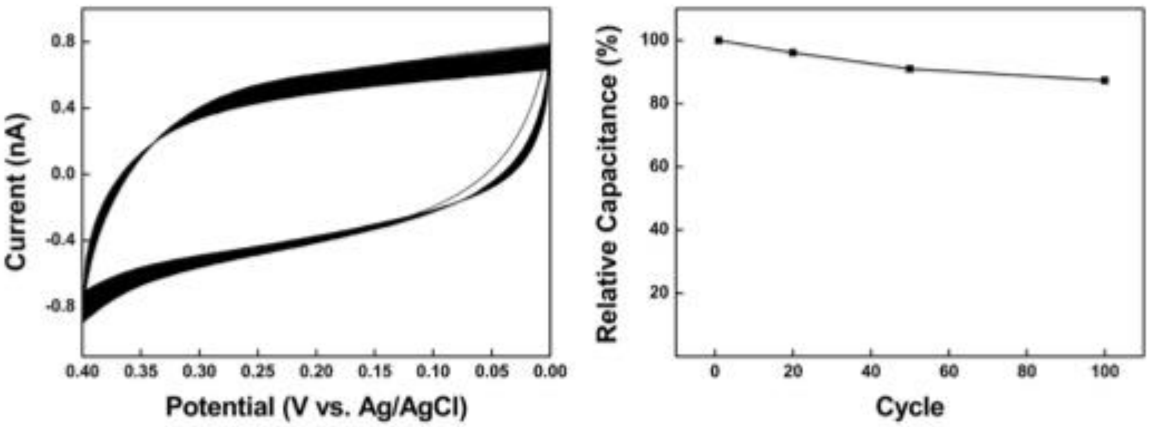

Figure S14. Supercapacitor charge-discharge cycle (left). The PEDOT NP based supercapacitor displayed little fading in performance after more than 100 continued cycles and greater than 2 h of use (right).

References

S1. L. Qian, Y. Zheng, J. Xue and P. H. Holloway, *Nat. Photonics*, 2011, **5**, 543-548.
S2. T. Earmme and S. A. Jenekhe, *J. Mater. Chem.*, 2012, **22**, 4660-4668.
S2. B.-K. Kim, A. Boika, J. Kim, J. E. Dick and A. J. Bard, *J. Am. Chem. Soc.*, 2014, **136**, 4849-4852.
S3. M. Culebras, C. M. Gómez and A. Cantarero, *J. Mater. Chem. A*, 2014, **2**, 10109-10115.
S4. W. Fan, C.-Y. Guo and G. Chen, *J. Mater. Chem. A*, 2018, **6**, 12275-12280.